

HIGH POWER IMPULSE MAGNETRON SPUTTERING OF THIN FILMS FOR SUPERCONDUCTING RF CAVITIES*

S. Wilde^{1,6}, R. Valizadeh¹, O.B. Malyshev¹, N.P. Barradas², E. Alves^{3,4}, G.B.G. Stenning⁵, A. Hannah¹, S. Pattalwar¹, B. Chesca⁶

¹ ASTeC, STFC Daresbury Laboratory, Warrington, UK

² C²TN, Centro de Ciências Tecnológicas e Nucleares, Portugal

³ IPFN, Instituto de Plasmas e Fusão Nuclear, Portugal

⁴ Laboratório de Aceleradores e Tecnologias de Radiação, Portugal

⁵ ISIS, STFC Rutherford Appleton Laboratory, Didcot, UK

⁶ Department of Physics, Loughborough University, Loughborough, UK

Abstract

The production of superconducting coatings for radio frequency cavities is a rapidly developing field that should ultimately lead to acceleration gradients greater than those obtained by bulk Nb RF cavities. The use of thin films made from superconductors with thermodynamic critical field, $H_C > H_C^{Nb}$, allows the possibility of multilayer superconductor – insulator – superconductor (SIS) films and also accelerators that could operate at temperatures above the 2 K typically used. SIS films theoretically allow increased acceleration gradient due to magnetic shielding of underlying superconducting layers [1] and higher operating temperature can reduce cost [2]. High impulse magnetron sputtering (HiPIMS) and pulsed DC magnetron sputtering processes were used to deposit NbN and NbTiN thin films onto Si(100) substrate. The films were characterised using scanning electron microscopy (SEM), x-ray diffraction (XRD), Rutherford back-scattering spectroscopy (RBS) and a four point probe.

INTRODUCTION

Superconducting radio frequency (SRF) cavity technology in particle accelerators is now reaching the limit of performance achievable with bulk Nb cavities [3]. Since superconducting properties for SRF are confined to a penetration depth of less than one micron [4] then superconducting thin-films offer an alternative to bulk Nb with the advantage of Cu substrates which have a factor of three higher thermal conductivity than Nb [5]. Multilayer SIS films have been suggested as a way to increase accelerating voltages further by utilising an increased first critical field (B_{c1}) for superconducting layers with $H_C > H_C^{Nb}$ and thickness (d) less than λ , to shield an underlying Nb layer (Fig. 1). Equation 1 shows that as film thickness and coherence length, ξ , get smaller then B_{c1} increases in the overlying superconducting layers [1]:

$$B_{c1} = \frac{2\phi_0}{\pi d^2} \ln \frac{d}{1.07\xi} \quad d < \lambda. \quad (1)$$

Another use of superconducting materials other than Nb is to reduce the surface resistance (R_s) of SRF cavities which allows for higher Q factors. Superconductors with $T_C > T_C^{Nb}$ have been shown to have a lower R_s than Nb at 4.2 K due to the fact that $R_s \propto e^{-T_C/T}$ [6]. It is also possible to reduce R_s further by combining higher T_C with as small a normal state low temperature resistivity as possible [7]. Operation at 4.2 K can provide reduced operational costs.

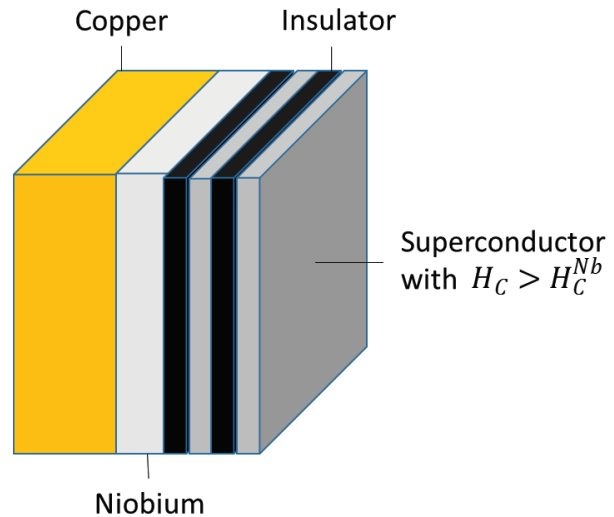


Figure 1: A schematic representation of an SIS multilayer film deposited on to Cu substrate.

The purpose of the present study is to deposit and then characterise a selection of NbN and NbTiN thin films that would be suitable for use in both SIS multilayer coatings or for operation in accelerators at 4.2 K. NbN was chosen for to its H_C of 0.23 T which is higher than the 0.2 T of Nb. NbN also has a high T_C of 17.3 K, small ξ of 2.9 nm and λ of 375 nm [6]. One drawback of NbN is its high normal state resistivity. NbTiN was therefore considered due to its smaller resistivity than NbN [2], higher T_C of 18 K, ξ of 3.8 nm [8] and λ of 150 nm. Films were deposited by reactive sputtering in a mixture of Kr and N₂ gas using three inch planar magnetrons utilising either an Ionautics

HiPSTER 1000 high impulse magnetron sputtering (HiPIMS) power supply or an Advanced Energy Pinnacle + pulsed DC power supply. The HiPIMS power supply creates a characteristic peak current which is up to two orders of magnitude higher than that of the pulsed DC. High current densities at the target allow for dense plasma with the possibility that sputtered atoms will become ionised [9]. Variable parameters during the experiment included the temperature of the substrate, N_2 partial pressure and the current supplied by the pulsed DC supply.

EXPERIMENTAL

Thin film samples were deposited onto Si (100) substrates in a mixture of both Kr and N_2 sputter gasses. The base pressure of the deposition chamber was $\sim 10^{-8}$ mbar and the pressure was maintained at 7×10^{-3} mbar during deposition. Each substrate was first prepared by cleaning in ultrasonic baths of acetone then IPA and finally rinsed in deionised water. All sample substrates were set to continuously rotate at 4 rpm during deposition at either room temperature or 385°C . NbN films were deposited for 3 hours by HiPIMS with an average current of 670 mA, peak current of 28 A, 1000 Hz repetition rate and 50 μs pulse length. N_2 partial pressure was then varied for each deposition so that the fraction of N_2 from the total gas pressure ranged 10 to 22%.

NbTiN films were deposited by dual magnetron sputtering. One magnetron fitted with a Nb target was powered by the HiPIMS power supply whilst another used a Ti target and the pulsed DC supply. NbTi films were first deposited to evaluate the correct settings of the pulsed DC supply. The HiPIMS supply maintained constant settings of 590 mA average current, 20 A peak current, 1000 Hz repetition rate and 50 μs pulse length. The pulsed DC supply was set to pulse at 350 kHz with a 50% duty cycle and an average current which varied from 0.4 to 1.2 A. It was found that 0.96 A provided by the pulsed DC supply produced NbTi with 34 atomic % Ti. 0.96 A was therefore considered the optimum current setting for the pulsed DC supply as the highest T_C in the literature occurs for films with fraction $Nb_{1-x}Ti_xN$ where $x = 0.34$ [8]. The optimum power settings were then maintained whilst N_2 partial pressure was varied as described for NbN.

Morphological characterisation of each film was performed by SEM, XRD and RBS. The SEM was used to measure the thickness of films and determine the film structure. XRD was used to determine the phase, preferred growth orientation and average grain size of films. RBS was used to quantify the elemental stoichiometry.

A four point probe was used to determine the superconducting transition temperature (T_C) followed by a calculation of the normal state DC resistivity.

NbN

T_C was measured for all samples deposited. NbN samples ranged in T_C from 7 to 16.1 K (Fig. 2).

NbN samples deposited with a substrate temperature of 385°C showed no superconductivity for samples deposited in Kr and N_2 atmosphere containing 10% partial pressure of N_2 or below. Samples became superconducting at 11% N_2 with the lowest T_C of 7 K. T_C of the NbN samples then increased with nitrogen partial pressure up to a maximum 16.1 K at 22% N_2 . It has previously been reported in the literature that increasing the temperature of the substrate during deposition will increase the T_C for NbN films [10]. Only two samples were deposited at room temperature and had reduced T_C of 10.7 and 10.3 K at partial pressures of 18 and 22% N_2 respectively.

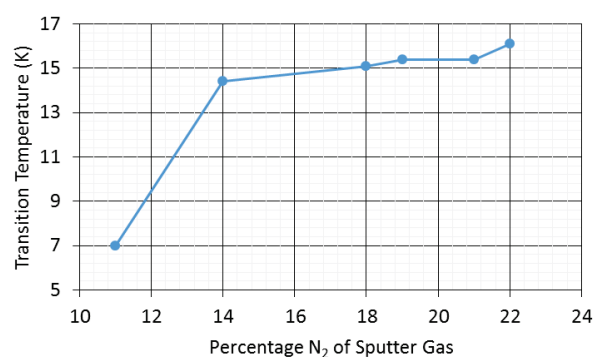


Figure 2: Transition temperatures for NbN thin films for varying nitrogen partial pressure. Substrate was maintained at 385°C .

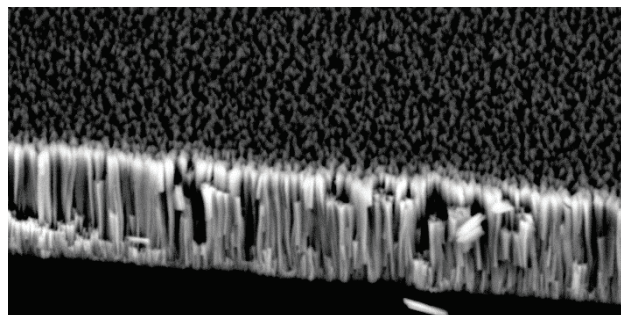


Figure 3: SEM image of a NbN thin film with thickness of 1500 nm and $T_C = 16.1$ K. Sample was deposited with 22% N_2 partial pressure with a substrate temperature of 385°C .

A selection of NbN samples were measured by SEM, XRD and RBS. Figure 3 was typical of the films deposited. NbN films were made up of columnar grains with voids. Voids were of a comparable size to the columnar structure. It has been previously reported that the high resistivity of NbN is due to the presence of metallic and gaseous voids [11]. The thicknesses of only two NbN films were measured by SEM. Both samples were deposited with a 22% N_2 partial pressure however one with a substrate heated to 385°C and the other

deposited at room temperature. The measurement of the thickness of the samples allowed the normal state DC resistivity at just above T_C to be calculated and resulted in $835 \pm 260 \mu\Omega\text{cm}$ for the high temperature deposition and $2094 \pm 650 \mu\Omega\text{cm}$ for the room temperature deposition. This result shows improved electrical performance for the substrate heated to 385°C when compared to a similar room temperature deposition.

All NbN samples which were measured by XRD showed the fcc phase with preferred growth orientation (111) (Fig. 4). The grain sizes of NbN films deposited at 385°C ranged from 43 to 51 nm with the largest grains of 51 and 48 nm occurring at N_2 partial pressures of 20 and 22% respectively. The grain size was measured for only one film deposited at room temperature. The film was deposited with 22% N_2 partial pressure and produced reduced grain size of 38 nm when compared to the same deposition conditions at 385°C .

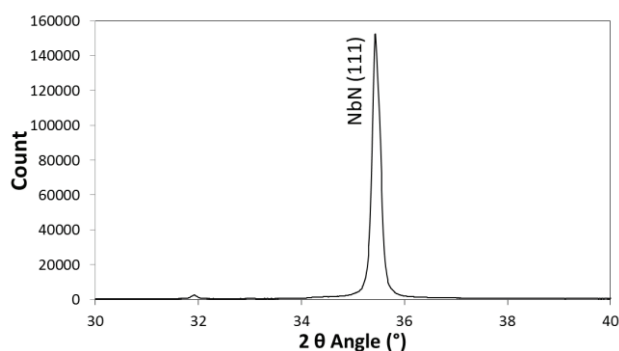


Figure 4: NbN thin film with $T_C = 16.1$ K. Sample was deposited with 22% N_2 partial pressure. XRD shows the fcc phase with preferred orientation (111).

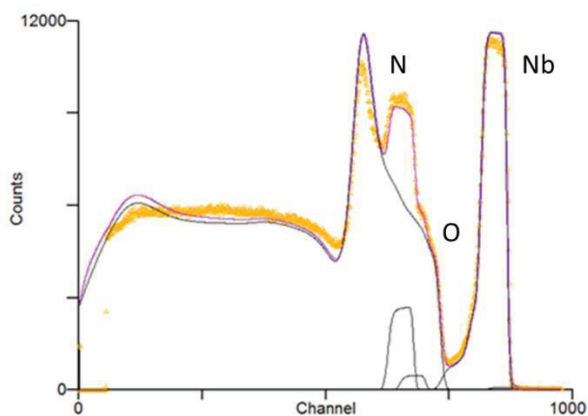


Figure 5: RBS data showing the ratio of N and Nb in the NbN film with highest $T_C = 16.1$ K. Measurement also shows the presence of O contamination. Measurement was performed using a hydrogen beam with 10° angle of incidence, 165° scattering angle and 25° exit angle.

RBS analysis of NbN samples show the presence of O contamination within the films (Fig. 5). The sample with the highest T_C of 16.1 K contained atomic percentages of

47.5% Nb, 42.6% N and 9.9% O. A possible source of O contamination could be outgassing from the unbaked vacuum system. Another possible source of O contamination is ex-situ post-deposition oxidation. SEM images showed a very rough surface with columnar grains that provide a large surface area for possible surface oxidation. There was no leak in the vacuum system. Further XPS measurements are planned to elucidate the origin of the O contamination.

NBTiN

All NbTiN samples were deposited at a substrate temperature of 385°C . Samples showed no superconductivity when deposited with an N_2 partial pressure of 11% or below. Samples were superconducting at a partial pressure of 14% N_2 upwards to 21% and the maximum T_C of 17.8 K occurring at 20% (Fig. 6).

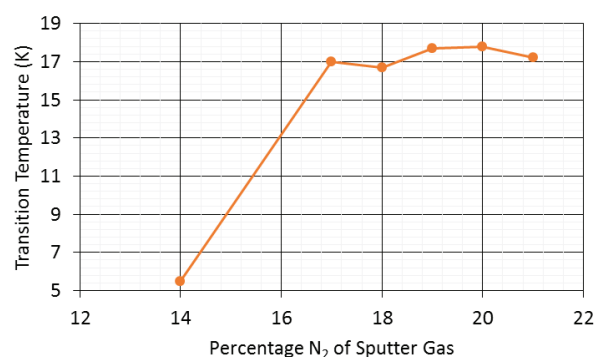


Figure 6: Transition temperatures of NbTiN thin films for varying nitrogen partial pressure. Substrate was maintained at 385°C .

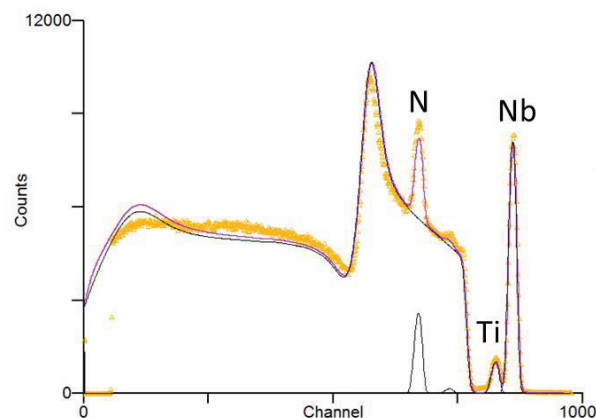


Figure 7: RBS data showing the elemental ratio of Nb, Ti and N in an NbTiN thin film. Measurement was performed using a hydrogen beam with 10° angle of incidence, 165° scattering angle and 25° exit angle.

RBS analysis showed no oxygen contamination in the two NbTiN films which were measured (Fig. 7). The correct stoichiometry for the highest T_C in the literature would correspond to 33% Nb, 17% Ti and 50% N. Our

films came closest to these values for the film deposited in a 20% partial pressure of N_2 and resulted in the highest T_C of 17.8 K (Table 1). It has been assumed that by altering the deposition conditions for future depositions then films can be produced with the desired ratios i.e. altering the current supplied to the Nb and Ti targets and the N_2 pressure accordingly to change the elemental percentages as required.

Table 1: Table showing the elemental composition of two NbTiN films deposited in N_2 partial pressures (N_2 P%) of 38 and 18%.

N_2 P%	T_C (K)	Nb (at.%)	Ti (at.%)	N (at.%)	O (at.%)
20	17.8	37.7	16.2	46.1	0
18	16.7	41.7	16.2	42.4	0

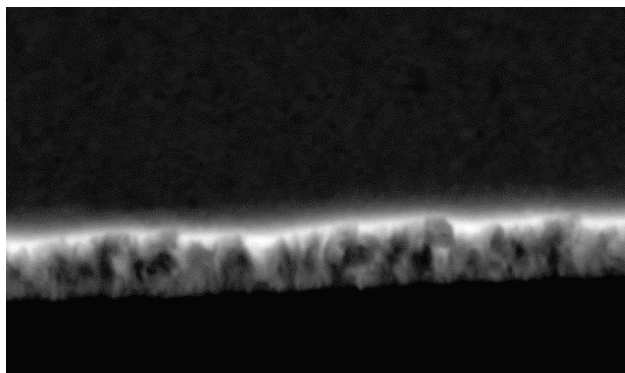


Figure 8: SEM image of a NbTiN thin film of thickness 350 nm and T_C of 17.8 K. Film appears to have a smoother surface and more densely packed grains than that of the NbN films.

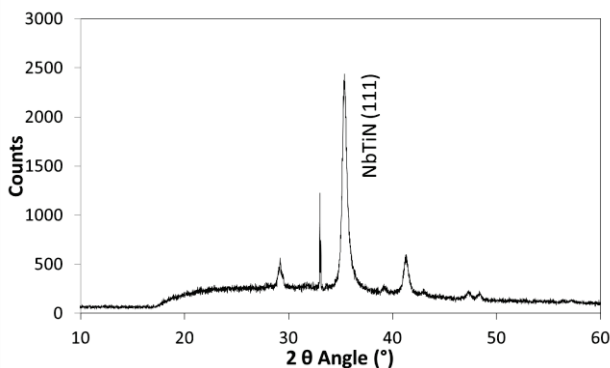


Figure 9: NbTiN thin film with T_C of 17.8 K. Sample was deposited with 20% N_2 partial pressure. XRD shows the fcc phase with preferred growth orientation (111).

SEM images of the NbTiN thin films show a much smoother surface than the NbN films (Fig. 8). NbTiN films appear to have more closely packed grains than the NbN samples. XRD measurements showed that NbTiN was formed with the same fcc phase and preferred orientation (111) as was seen in the NbN films (Fig. 9). Average NbTiN grain sizes were 12 nm for a film deposited in 18% partial pressure of N_2 and 16 nm for 20% N_2 . The addition of Ti to the film contributes a mismatch in atomic size when compared to Nb therefore

forming smaller grains than NbN. A reduction in grain size for NbTiN may have allowed the formation of a denser structure.

The normal state DC resistivity was calculated for the only NbTiN sample with a measured thickness. This sample showed the highest T_C of 17.8 K and the corresponding resistivity was $45 \pm 7 \mu\Omega\text{cm}$. The measured NbTiN resistivity was an order of magnitude improvement over the resistivity measured for the highest T_C NbN sample.

CONCLUSIONS

The study set out to use HiPIMS to produce NbN and NbTiN thin films with comparable or higher T_C to those presented in the literature to date. NbN films were produced first and showed a maximum T_C of 16.1 K and a normal state DC resistivity of $835 \pm 260 \mu\Omega\text{cm}$. RBS measurements of these films showed the films to be non-stoichiometric and contained some contamination by O. Possible origins of the contamination are outgassing from the unbaked vacuum system or ex-situ post deposition surface oxidation.

NbTiN films were produced in order to test their increased T_C and superior electrical properties when compared to NbN. Our results showed a highest T_C of 17.8 K and a normal state DC resistivity of $45 \pm 7 \mu\Omega\text{cm}$. The NbTiN film had an order of magnitude lower resistivity than that of the best NbN sample. This sample was close to stoichiometric ratios reported previously in the literature to achieve the highest T_C .

REFERENCES

- [1] A. Gurevich, Appl. Phys. Lett. **88**, 012511 (2006).
- [2] A. M. Valente-Feliciano et al., TUP088, Proc. SRF2013, <http://jacow.org/>
- [3] P. Kneisel et al., TPPT076, Proc PAC2005, <http://jacow.org/>
- [4] W. M. Roach et al., PRST-AB **15**, 062002 (2012).
- [5] C. James et al., IEEE Trans. Appl. Supercond. **23**, 3500205 (2013).
- [6] S. Posen and M. Liepe, WEZBA1, Proc. PAC2013, <http://jacow.org/>
- [7] V. Palmieri, "New materials for superconducting radiofrequency cavities," RFSC-Limits (2004).
- [8] L. Yu et al., IEEE Transactions on Applied Superconductivity **15**, 44 (2005).
- [9] A. Anders et al., J. Appl. Phys. **102**, 113303 (2007).
- [10] W. M. Roach et al., Superconductor Science and Technology **25**(12), 125016 (2012).
- [11] A. M. Valente-Feliciano et al., THPO074, Proc SRF2011, <http://jacow.org/>